

Paper:

Neuro-Based Position and Force Hybrid Control of Six-Legged Walking Robot

Qing-jiu Huang* and Kenzo Nonami**

*Artificial System Science, Graduate School of Science and Technology, Chiba University,
1-33 Yayoi-cho, Inage-ku, Chiba, 263-8522 Japan
E-mail: huang@mec2.tm.chiba-u.ac.jp

**Department of Electronics and Mechanical Engineers, Faculty of Engineers, Chiba University,
1-33 Yayoi-cho, Inage-ku, Chiba, 263-8522 Japan.
E-mail: nonami@meneth.tm.chiba-u.ac.jp

[Received May 30, 2002; accepted June 11, 2002]

We propose a six-legged walking robot having two manipulators which offers added stability, mobility, and functionality. We studied neuro-based position and force hybrid motion control for walking on irregular terrain. Comparison with conventional position and force hybrid control demonstrates the high efficiency of the proposed neuro-based position and force hybrid control. The neuro-based position and force hybrid control includes six-axis force sensors in each leg, which provide control vertically, i.e., in the direction of gravity, and in the walking direction. This platform has proven to be very useful on irregular terrain including obstacles of random height and random position. Consequently, autonomous stable walking in an unknown environment has been realized through experiments.

Keywords: six-legged walking robot, neuro-based position and force hybrid control, nonlinear control, irregular terrain walking, autonomous stable walking

1. Introduction

A legged walking robot, such as a single-legged (hopping machine), two-legged, four-legged, six-legged, or eight-legged robot, must have at least 4 legs to realize static stable walking. A legged walking robot has an advantage over a wheeled robot, in that it can move on irregular terrain and avoid obstacles. Therefore, legged robots are expected to find application to dangerous working environments, such as in nuclear reactors, on extraterrestrial planets, in mine fields, and under limited working conditions.¹⁻⁷⁾

Our research group had developed a six-legged walking robot for mine detection. Previously, we built and reported on COMET-I and COMET-II.⁸⁾ In particular, in view of exploiting the advantages of legged walking robots, we concentrate our study on irregular terrain walking, mine detection, mine marking, mine mapping, and related functions. Position and force hybrid control is known to be efficient for irregular terrain walking by a

legged walking robot. However, constructing a mathematical model of a multilegged walking robot and designing a model-based control are very difficult, because of the complexity of such a large-scale nonlinear system. Constructing a mathematical model for a legged walking robot is especially difficult, because of the dynamics of unpredictable conditions, such as unknown changes resulting from collision and viscoelasticity between foot and ground. A conventional position and force hybrid control is designed on a turning method based on rule of thumb and trial and error, not based on a mathematical model, but preventing realization of good control performance. Of course, because tracing performance of conventional hybrid control depends on feedback gain matrices, performance is improved if proper gain can be obtained, at the expense of a great amount of time. However, in practice, three unknown gains exist on the diagonal of each of the four gain matrices in the case of one leg, which consists of three joints. It is very difficult to determine the twelve unknown gains. , when robot walking in unknown environment, it is impossible to tune these twelve gains, so that it is impossible to realize the autonomous walking by using the conventional position and force hybrid control. Therefore, in the present study we seek to improve control performance by means of building an adaptive learning control that does not rely on a mathematical model for position and force hybrid control. The neuro learning method is an efficient method for this purpose.

Neuro-based nonlinear control has been applied in the field of control,⁹⁻¹¹⁾ but, to the best of our knowledge, no study has been conducted on applying neuro-based position and force hybrid control to a legged walking robot. Therefore, we have proposed a new control for a robot walking on irregular terrain; namely, a neuro-based position and force hybrid control which enables a robot to realize autonomous walking by self-learning. Specifically, first we designed a decentralized position and force hybrid control for each joint of each leg by means of a turning method utilizing rule of thumb and trial and error. Next, we designed hierarchical control, which consists of a centralized neuro-based controller and a decentralized





Fig. 1. Overview of six-legged walking robot with two manipulators.

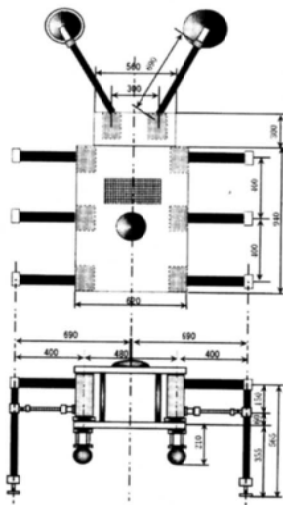


Fig. 2. Size of six-legged walking robot.

position and force hybrid control for three joints of each leg. Furthermore, by using this neuro-based controller, we obtained the dynamics of environment after the robot walking learning, thereby improving control performance of position and force hybrid control. Particularly, by employment of six-axis force sensors, the proposed control provides control not only vertically; i.e., in the direction of gravity, but also in the walking direction. Therefore, when the swing leg comes into contact with an obstacle in the walking direction, robot can avoid the obstacle by stepping over it. Tracing performance for target value is improved by adjusting the bias of a sigmoidal function in the neuro-based algorithm. Comparison with conventional position and force hybrid control reveals that the proposed neuro-based position and force hybrid control is highly efficient.

2. Overview of Robot

Figure 1 shows the overall six-legged walking robot,

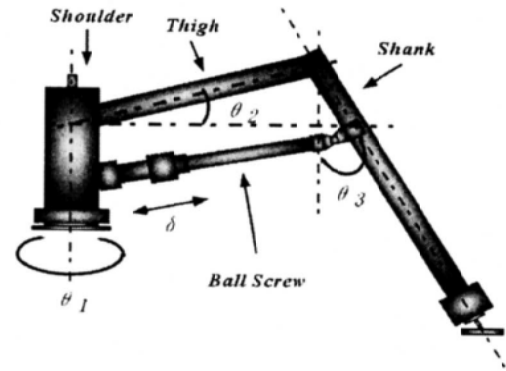


Fig. 3. Configuration of each leg.

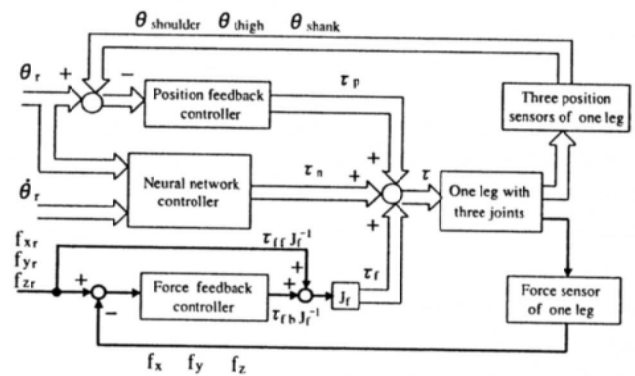


Fig. 4. Control with neuro-based position/force hybrid controller.

and Fig.2 shows its dimensions.¹²⁾ The robot has six three-joint legs, each consisting of a shoulder, a thigh, and a shank. Total weight is about 120 kgf, overall width is about 1300 mm, and body height is about 600 mm. Walking speed on structured ground is about 150 m/h. The present study employs a six-legged walking robot in which each leg has 3 degrees-of-freedom (DOF), to ensure more stable walking on irregular terrain. Fig.3 shows the configuration of each leg. The leg mechanism uses a parallel link for the thigh, and the ball joint of the parallel link pivots the shank. A power generator supplies power sufficient for four hours' continuous operation, and an external power supply supplies power for long-time operation.

3. Neuro-Based Position and Force Hybrid Control

3.1. Structure of Control

Figure 4 depicts the control for each leg. Six block diagrams shown in Fig.4, because the six legs have identical controls represent the control for the entire robot.

The control has three components. The first component is a position control with a PD feedback controller for each joint, and the second component is a force control using a feedforward controller and a PD feedback controller. The first component and the second component constitute a conventional position and force hybrid control. The third component, which is designed based on neuro learning for attaining ideal control performance without use of a correct mathematical model of the leg, is a position and force hybrid control that uses an inverse-function centralized control compensator for the three joints of one leg. The third component and the hierarchical control structure shown in Fig.4 are the concepts that are newly proposed in our study.

Figure 5 shows an enlarged view of the neuro-based compensator shown in Fig.4. Here, we introduce briefly the method of obtaining an inverse-function centralized control compensator for the three joints of one leg. As shown in Fig.4, a man-made neuro-based compensator is added to the sum of position feedback controller and force feedback controller. Input signals of the neuro-based compensator are target orbit for three joints of one leg θ_r ($i=1 \dots 3$) and its first order differential $\dot{\theta}_r$ ($i=3 \dots 6$). The output signal of the neuro-based compensator τ_{n_k} ($k=1 \dots 3$), which is combined with the output signal of position control τ_{p_k} ($k=1 \dots 3$) and the output signal of force control τ_{f_k} ($k=1 \dots 3$), is transmitted to each joint as a control input signal. Here, error signals of the neuro-based compensator are τ_{p_k} and τ_{f_k} , and teacher signals are the input torque τ_k , which is the sum of τ_{n_k} , τ_{p_k} and τ_{f_k} . After learning with the above method, this neuro-based compensator can sense the nonlinear properties of the controlled object robot such as slip and collision between the robot foot and the floor, and an inverse dynamics of actual motion can be obtained. The construction of the neuro-based compensator has an input layer, a middle layer and an output layer, as shown in Fig.5. The weight between the input layer and the middle layer is W_{ij} ($j=1 \dots 12$), and that between the middle layer and the output layer is V_{jk} . In consideration of learning time and learning efficiency, providing the middle layer with 12 units is appropriate when real-time learning is to be performed. , tracing performance for target value is improved by adjusting the bias of a sigmoidal function in this neuro-based algorithm. Both the design method and the algorithm of the neuro-based compensator are discussed in section 3.3.

Figure 6 shows an example of irregular terrain. A walking robot, which is to move on such an unstructured ground surface generally, requires a hybrid control, which provides position and force control. In Fig.6, which depicts all legs as being in the support phase, the force of each leg vertically z equals the specified force for stabilizing attitude. Position control is applied to x and y directions.

In the swing phase of a leg, as shown in Fig.7, when the height of an obstacle is greater than the height from

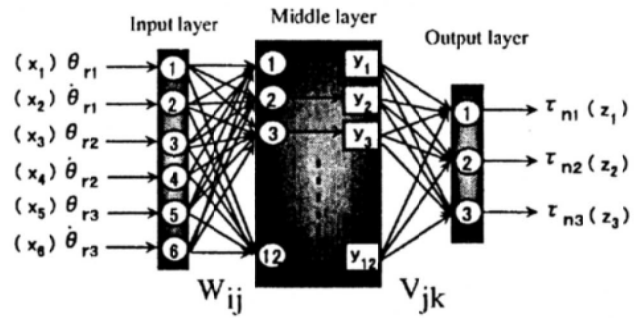


Fig. 5. NN Structure.

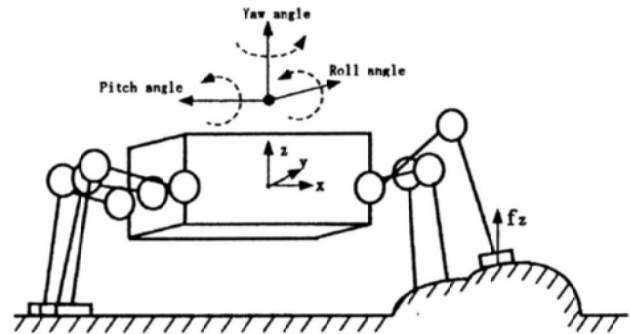


Fig. 6. Walking on irregular terrain with neuro-based position and force hybrid control.

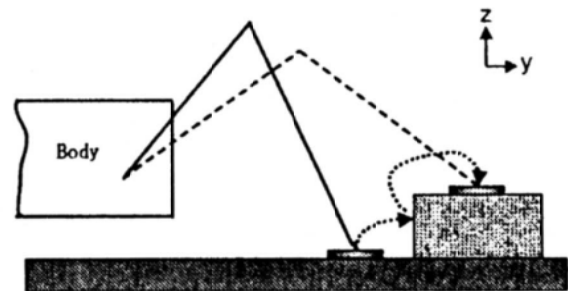


Fig.7. Avoidance for high obstacle.

the ground to the swing leg of the robot, position control is performed in the z direction, whereas force control is in the y direction; that is, the walking direction. As soon as the leg comes into contact with the obstacle in the walking direction, the leg accepts a force signal, and in response the swing leg retreats and rises again in an effort to step over the obstacle. Particularly, in the case where the center of gravity of the robot is raised, the swing leg can be raised higher to step over the higher obstacle. In this manner, the robot can walk over obstacle up to 15cm in our study.

3.2. Conventional Position and Force Hybrid Control

First, conventional position and force hybrid control are introduced, where $\theta_r = [\theta_{r1}, \theta_{r2}, \theta_{r3}]^T$ is the reference position, $f_r = [f_{r1}, f_{r2}, f_{r3}]^T$ is the reference force, and $\theta_i = [\theta_1, \theta_2, \theta_3]^T$ and $f_i = [f_x, f_y, f_z]^T$ are the present position

and the present force. Position error and force error are expressed as

$$\theta_{e_i}(t) = (I - T)(\theta_{r_i}(t) - \theta_i(t)) \dots \dots \dots (1)$$

$$f_{e_i}(t) = T(f_{r_i}(t) - f_i(t)) \dots \dots \dots (2)$$

Where, T is the transform matrix concerning position and force.

$$T = \begin{bmatrix} 1 & 0 & 0 \\ 0 & 0 & 0 \\ 0 & 0 & 0 \end{bmatrix} \quad (f_x > 0, \text{ swing phase}) \dots \dots (3)$$

$$T = \begin{bmatrix} 0 & 0 & 0 \\ 0 & 1 & 0 \\ 0 & 0 & 0 \end{bmatrix} \quad (f_y > 0, \text{ swing phase}) \dots \dots (4)$$

$$T = \begin{bmatrix} 0 & 0 & 0 \\ 0 & 0 & 0 \\ 0 & 0 & 1 \end{bmatrix} \quad (f_z > 0, \text{ support phase}) \dots \dots (5)$$

$$T = \begin{bmatrix} 0 & 0 & 0 \\ 0 & 0 & 0 \\ 0 & 0 & 0 \end{bmatrix} \quad (f_x = 0, f_y = 0, f_z = 0, \text{ swing phase}) \dots \dots (6)$$

Using vector J_f for θ_i , the relation between torque and force is given by

$$J_f = \begin{bmatrix} 0 & J_{f12} & 0 \\ 0 & 0 & J_{f23} \\ J_{f31} & 0 & 0 \end{bmatrix}$$

$$\begin{aligned} J_{f12} &= -l_s \cos(\theta_3) \\ J_{f23} &= -(l_s \sin(\theta_3) + l_t \cos(\theta_2)) \\ J_{f31} &= -(l_t \cos(\theta_2) + l_s \sin(\theta_3) \cos(\theta_1)) \end{aligned} \dots \dots \dots (7)$$

$$\tau_e(t) = J_f f_{e_i}(t) \dots \dots \dots (8)$$

In Eq.(7), l_t is the length of the thigh, and l_s is the length of the shank. To compensate position error and force error, a torque τ_p and τ_{fb} should be applied, as follows:

$$\tau_p(t) = K_{p_p} \theta_{e_i}(t) + K_{p_d} \dot{\theta}_{e_i}(t) \dots \dots \dots (9)$$

$$\tau_{fb}(t) = K_{f_p} \tau_e(t) + K_{f_d} \dot{\tau}_e(t) \dots \dots \dots (10)$$

where K_{p_p} , K_{p_d} , K_{f_p} , are feedback gain matrices. Hybrid

control torque is expressed as follows:

$$\begin{aligned} \tau(t) &= \tau_p(t) + \tau_f(t) \\ &= \tau_p(t) + \tau_{pb}(t) + \tau_{ff}(t) \\ &= K_{p_p} \theta_{e_i}(t) + K_{p_d} \dot{\theta}_{e_i}(t) + K_{f_p} \tau_e(t) + K_{f_d} \dot{\tau}_e(t) + J_f T f_r \\ &= K_{p_p} \theta_{e_i}(t) + K_{p_d} \dot{\theta}_{e_i}(t) + J_f (K_{f_p} f_{e_i}(t) + K_{f_d} \dot{f}_{e_i}(t) + T f_r) \end{aligned} \dots \dots \dots (11)$$

This force control rule is based on the proposal of Raibert and Craig.¹³⁾

3.3 Neuro-based Position and Force Hybrid Control

Equation (11) expresses the control input of conventional position and force hybrid control. However, because the four feedback gain matrices K_{p_p} , K_{p_d} , K_{f_p} and K_{f_d} in Eq.(11) are obtained by rule of thumb and trial and error, good control performance cannot be realized. In this study, we propose a new position and force hybrid control that is based on a neural network, which can realize good control performance without a correct mathematical model of the leg.

Using the hybrid control input $\tau_p + \tau_{fb}$, the neuro controller can determine the actual control input by feedback error learning. Eq.(12) expresses the desired control input of the neuro controller for each motor.

$$\tau_d(t) = V_{jk}^T y_j (W_{ij}^T x_i) + K_{p_p} \theta_{e_i}(t) + K_{p_d} \dot{\theta}_{e_i}(t) + J_f (K_{f_p} f_{e_i}(t) + K_{f_d} \dot{f}_{e_i}(t)) \dots \dots \dots (12)$$

The input layer x_i ($i=1 \dots 6$) shown in **Fig.5** consists of the position and velocity of reference trajectories of the three joints of one leg. The output layer z_k ($k=1 \dots 3$) consists of the input torque τ_n for three motors of the one leg as determined from inverse dynamics of the neuro compensator.

The relations among units of layers are as follows:

$$x_i(K) = \theta_{r_i}(K), \dot{\theta}_{r_i}(K), \dots, \theta_{r_i}(K), \dot{\theta}_{r_i}(K) \dots (13)$$

$$y_j(K) = f \left(\sum_i W_{ij}(K) x_i(K) \right) \dots \dots \dots (14)$$

$$\begin{aligned} z_k(K) &= \tau_{n_k}(K) = f \left(\sum_j V_{jk}(K) y_j(K) \right) \\ i &= 1 \dots 6, j = 1 \dots 12, k = 1 \dots 3 \end{aligned} \dots \dots \dots (15)$$

where, the sigmoidal function is defined as follows:

$$f(u(K)) = \frac{2}{1 + e^{-(u(K)+b(K))}} - 1 \dots \dots \dots (16)$$

where, $b(K)$ is the item for improving learning ability.

The error convergence equation derived by the method of steepest descent is given by:

$$\begin{aligned} E(K) &= \frac{1}{2} \sum_1^k (\tau_{n_k}(K) - \tau_{d_k}(K))^2 \\ &= \frac{1}{2} \sum_1^k (-\tau_{p_k}(K) - J_f(\tau_{f_k}(K) - Tf_{z_k}(K)))^2 \\ &= \frac{1}{2} \sum_1^k (-K_{p_p} \theta_{e_i}(t) - K_{p_d} \dot{\theta}_{e_i}(t) - J_f(K_{f_p} f_e(t) - K_{f_d} \dot{f}_e(t)))^2 \\ &\dots \dots \dots (17) \end{aligned}$$

The relations between weights W_{ij} , V_{jk} and error E are as follows:

$$\frac{dV_{jk}}{dt} = -\frac{\partial E}{\partial V_{jk}} \dots \dots \dots (18)$$

$$\frac{dW_{jk}}{dt} = -\frac{\partial E}{\partial W_{jk}} \dots \dots \dots (19)$$

Error signal E is differentiated by weighting W_{ij} and V_{jk} ,

$$\frac{\partial E}{\partial V_{jk}} = \frac{\partial E}{\partial z_k} \frac{\partial z_k}{\partial V_{jk}} \dots \dots \dots (20)$$

$$\frac{\partial E}{\partial W_{ij}} = \frac{\partial E}{\partial z_k} \frac{\partial z_k}{\partial y_j} \frac{\partial y_j}{\partial W_{ij}} \dots \dots \dots (21)$$

In this case, $z_k(K)$, $y_j(K)$, $E(K)$ can be solved from Eqs.(14), (15), and (17).

According to Eqs.(18), (19), (20), and (21), renewing equations of weights W_{ij} , V_{jk} are as follows:

$$\Delta V_{jk}(K) = -\varepsilon \delta_{2k}(K) y_j(K) + \alpha \Delta V_{jk}(K-1) \dots (22)$$

$$\Delta W_{ij}(K) = -\varepsilon \delta_{1j}(K) x_i(K) + \alpha \Delta W_{ij}(K-1) \dots (23)$$

$$\begin{aligned} \delta_{2k} &= -\frac{1}{2} (-K_{p_p} \theta_{e_i}(t) - K_{p_d} \dot{\theta}_{e_i}(t) - J_f(K_{f_p} f_e(t) - K_{f_d} \dot{f}_e(t))) (1 - \tau_{n_k}(K))^2 \\ &\dots \dots \dots (24) \end{aligned}$$

$$\delta_{1j}(K) = \frac{1}{2} (\sum_1^k \delta_{2k}(K) V_{jk}(K)) (1 - y_j(K))^2 \dots (25)$$

$$V_{jk}(K) = V_{jk}(K-1) + \Delta V_{jk}(K) \dots \dots \dots (26)$$

$$W_{ij}(K) = W_{ij}(K-1) + \Delta W_{ij}(K) \dots \dots \dots (27)$$

To improve the performance in tracing target value, bias $b(K)$ is introduced into the sigmoidal function $f(u(K))$ of Eq.(16). The Adjustment method for bias is the same as that for obtaining the weighting $W_{ij}(K)$ and $V_{jk}(K)$ by the method of steepest descent. First, the relationships between the input layer and the middle layer, and the sigmoidal function are

$$y_j(K) = f_1 \left(\sum_i W_{ij}(K) x_i(K) \right) \dots \dots \dots (28)$$

$$f_1(u_1(K)) = \frac{2}{1 + e^{-(u_1(K)+b_1(K))}} - 1 \dots \dots \dots (29)$$

The relationships between the middle layer and the output layer, and the sigmoidal function are

$$u_{n_k}(K) = f_2 \left(\sum_j V_{jk}(K) y_j(K) \right) \dots \dots \dots (30)$$

$$f_2(u_2(K)) = \frac{2}{1 + e^{-(u_2(K)+b_2(K))}} - 1 \dots \dots \dots (31)$$

where, bias $b_2(K)$ can be obtained from Eqs.(30) and (31):

$$\begin{aligned} \Delta b_2(K) &= -\varepsilon \frac{\partial E}{\partial b_2} + \alpha \Delta b_2(K-1) \\ &= -\varepsilon \frac{\partial E}{\partial u_{n_k}} \frac{\partial u_{n_k}}{\partial b_2} + \alpha \Delta b_2(K-1) \\ &= -\varepsilon \frac{\partial E}{\partial u_{n_k}} \frac{\partial f_2}{\partial b_2} + \alpha \Delta b_2(K-1) \\ &\dots \dots \dots (32) \end{aligned}$$

$$b_2(K) = b_2(K-1) + \Delta b_2(K) \dots \dots \dots (33)$$

and bias $b_1(K)$ can be obtained from Eqs.(28) and (29):

$$\begin{aligned} \Delta b_1(K) &= -\varepsilon \frac{\partial E}{\partial b_1} + \alpha \Delta b_1(K-1) \\ &= -\varepsilon \frac{\partial E}{\partial u_{n_k}} \frac{\partial u_{n_k}}{\partial y_j} \frac{\partial y_j}{\partial b_1} + \alpha \Delta b_1(K-1) \\ &= -\varepsilon \frac{\partial E}{\partial u_{n_k}} \frac{\partial f_2}{\partial y_j} \frac{\partial f_1}{\partial b_1} + \alpha \Delta b_1(K-1) \\ &\dots \dots \dots (34) \end{aligned}$$

$$b_1(K) = b_1(K-1) + \Delta b_1(K) \dots \dots \dots (35)$$

Where, K is the renewing frequency ε , which is called

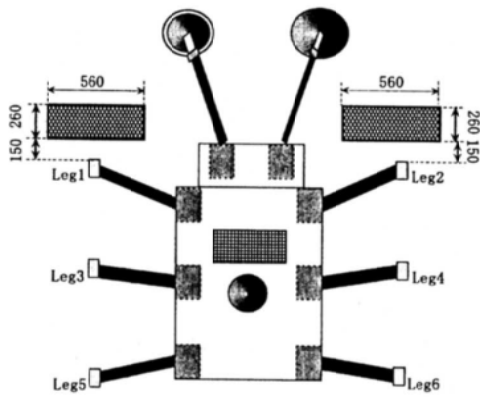


Fig. 8. Experimental condition.

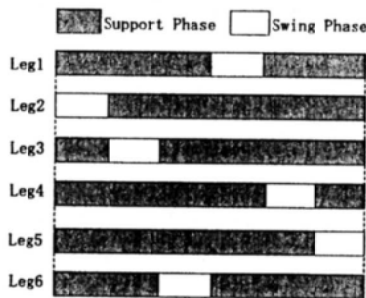


Fig. 9. Walking pattern.

learning rate, α is a constant falling within the range of 0 to 1. α is a small positive constant. Let the initial value of the output signal of the neuro compensator be zero, and let all of the weightings V_{jk} between the middle layer and the output layer also be zero. The weightings W_{ij} between the input layer and the middle layer are initialized randomly. With these initial values of parameters W_{ij} and V_{jk} , the parameters can be renewed by self-learning of Eqs.(23)-(27) and Eqs.(32)-(35).

4. Experiment

4.1. Experimental Conditions

An experiment was performed on an unstructured ground surface as shown in Fig.8. Walk gait is shown in Fig.9. This walk gait, which is called pentapod, is a walking pattern including only one swing leg and five support legs. Walking cycle for a single leg is 36s, average moving speed is approximately 0.0083m/s, and walking space is 0.30m. If obstacle height is excessive, in the initial period of learning the robot will yield a large error between the desired target value and the actual value of each joint; therefore, we selected a relatively low obstacle height of 6cm.

In relation to learning frequency, in 1 learning cycle of 216s, all the robot legs pass over an obstacle. In 1 learning cycle sampling frequency is 10800, and renewal fre-

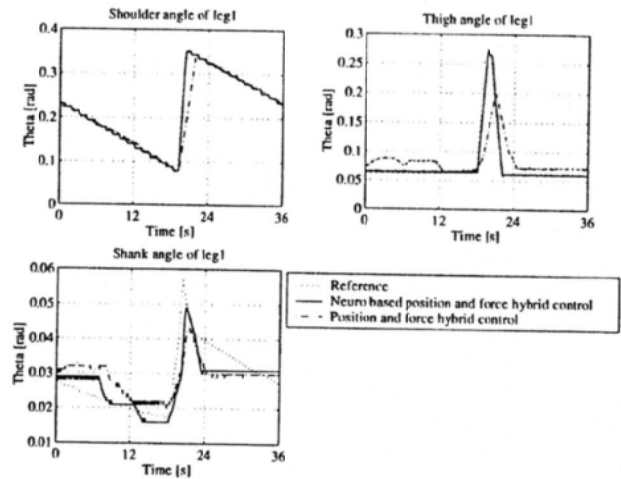


Fig. 10. Position reference response of Leg1.

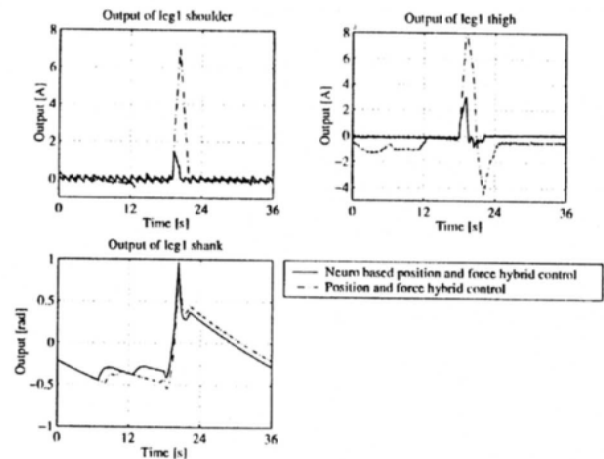


Fig. 11. Control input of Leg1.

quency of weighting is also 10800. Computer hardware used for the experiment includes an Intel Pentium II CPU (450Hz, 128MB). Although the fastest sampling time for the program is 20ms, we set sampling time to 25ms, to provide a buffer for calculation time. The error convergence status of learning is judged from the error convergence between system response and target value. In this study, after 20 learning cycles, the error between system response and target value is sufficiently small and approximates a constant; therefore, we treat the 20th learning cycle as the final convergence learning cycle.

4.2. Tracing Performance for Position Target Value on Hybrid Control

In this study, we compare conventional position control with neuro-based position control. Some studies, such as Ref.11), have reported the excellent orbit tracing performance of neuro-position control, and we obtained the same result. Fig.10 shows the target values (dotted lines), responses of neuro position control (solid lines), and responses of position control (broken line) of three joints of Leg 1 during walking over a structured ground surface.

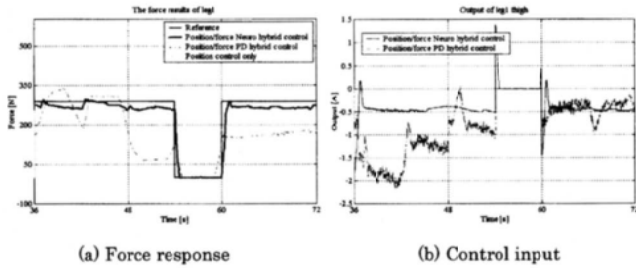


Fig. 12. Experimental results for Leg1.

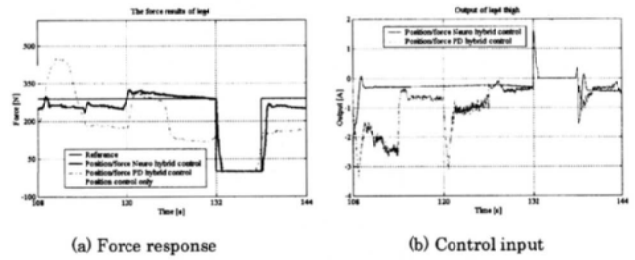


Fig. 15. Experimental results for Leg4.

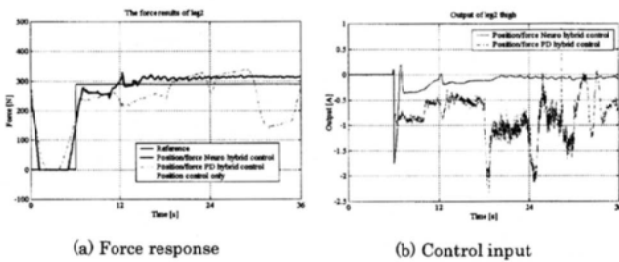


Fig. 13. Experimental results for Leg2.

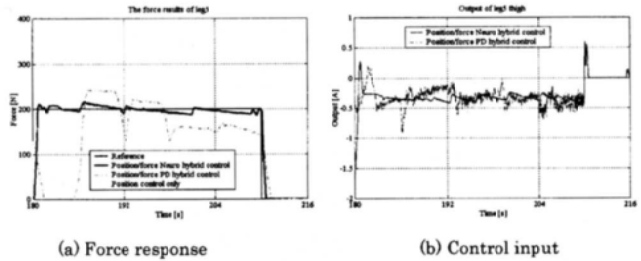


Fig. 16. Experimental results for Leg5.

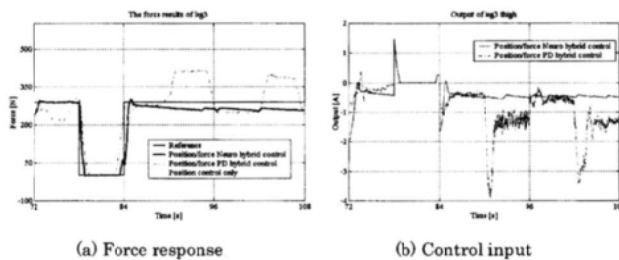


Fig. 14. Experimental results for Leg3.

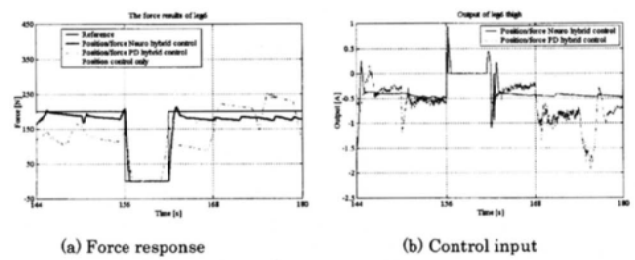


Fig. 17. Experimental results for Leg6.

The results suggest that neuro position control of all three joints attains excellent performance for tracing the target value. The results for the other five legs are the same as those for Leg 1 (omitted due to space limitations). Fig.11 shows the control input corresponding to Fig.10. The results show that the control input of neuro position control is small, and the vibration of the control input is constrained. Also, in the case of neuro position control, tracing performance for target value is excellent, enabling realization of the desired walking space of 30cm. However, in the case of position control, the desired walking space cannot be realized, and is no more than 28cm.

4.3. Tracing Performance for Force Target Value on Hybrid Control

In this section, we introduce the experimental results for the neuro-based position and force hybrid control proposed in this study.

Figures 12-17, show, for legs 1 to 6, force target values (dotted lines), responses of neuro-based position and

force hybrid control (bold solid lines), responses of conventional position and force hybrid control (broken lines), and responses of solely position control (solid line). Fig.12(a) shows that the response of neuro-based position and force hybrid control most closely approximates the force target value, followed by response of conventional position and force hybrid control, and response of solely position control. Tracing performance for force target value of neuro-based position and force hybrid control exceeds 92%, whereas that of conventional position and force hybrid control reaches only 50%. Of course, because tracing performance of conventional hybrid control depends on feedback gain matrices, performance is improved if proper gain can be obtained, at the expense of a great amount of time. However, in practice 3 unknown gains exist on the diagonal of each of the four gain matrices K_{pp} , K_{pv} , K_{fp} and K_{fd} in Eq.(11). It is very difficult to determine the twelve unknown gains. Therefore, the new algorithm proposed in this study is required for the multilegged walking robot. Fig.12(b) shows the control input

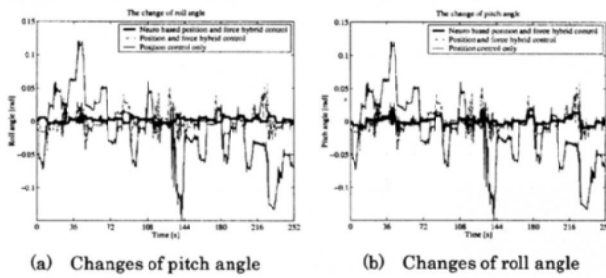


Fig. 18. Changes in posture angle of body.

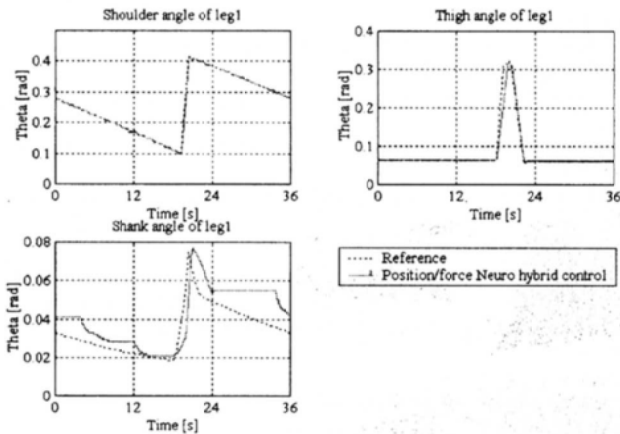


Fig. 19. Position reference response of Leg1.

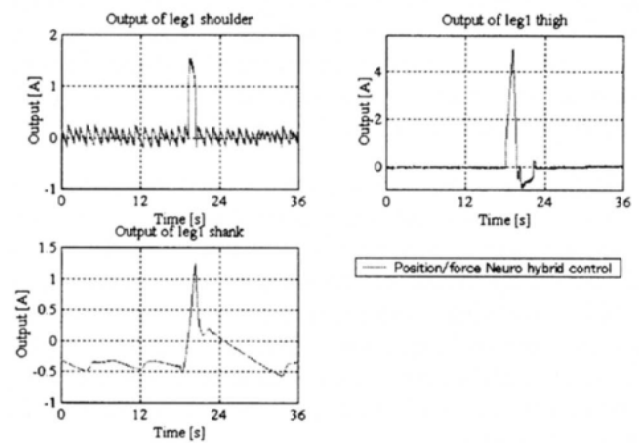


Fig. 20. Control input of Leg1.

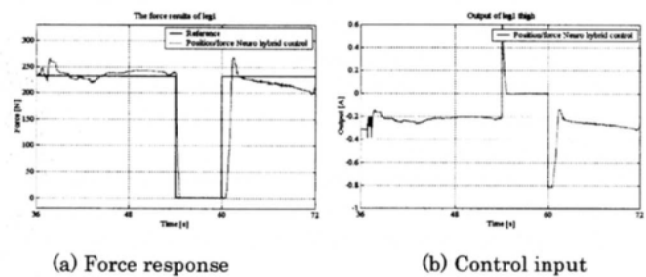


Fig. 21. Experimental results for Leg1.

corresponding to (a), in comparison with conventional hybrid control; in neuro-based hybrid control the vibration of control input is almost zero, and the control input itself is quite small. In other words, Fig.12 shows that control input is very small and that control performance is excellent.

Figure 13 shows the experimental results for Leg 2, which shows the same tendency as does control performance of Leg 1. Fig.13(a) shows that the response of conventional hybrid control deviates from the target value near 30s, resulting in a large posture change of pitch angle and roll angle of the robot, as shown in Fig.18(a) and (b). Also, in neuro-based hybrid control, posture change of the robot is restrained. Figures 14-17 are the same as Figs.12 and 13.

4.4. Walking on Unstructured Ground Using Generalization Ability, and Projected Work

As soon as the neuro-based position and force hybrid control is built, the desired output can be obtained for an arbitrary target value pattern. This is called "generalization ability" of neural network learning. Here, an unstructured ground surface walking experiment was conducted against a unknown walking orbit with obstacles of height ranging from 6 cm to 20 cm, by using 20 learning cycle weighting. Figures 19-21 show the experimental results for Leg 1. Figs.19 and Fig.21(a) show that the tracing

performances for position and force target orbit are excellent, even in the absence of learning.

The experimental results show that if the portion of the foot bottom of the robot that comes into contact with the obstacle is less than half the area of the foot bottom, the leg falls from the obstacle to the ground. At that time, with force control of f_z , although robot will not fall, its foot will receive impact. In this case, landing position should be changed by controlling moment M_x , M_y in the foot. , posture control based on neuro-based position and force hybrid control should be effective for walking on a slope and for unstable walking, such as dynamic walking.

5. Conclusions

We proposed a new control for a walking robot walking on an unstructured ground surface. This is a neuro-based position and force hybrid control, with which robot can realize autonomous walking by self-learning. Particularly, by employment of six-axis force sensors, the proposed control provides control not only vertically; i.e., in the direction of gravity, but also in the walking direction. Therefore when the swing leg comes into contact with an obstacle in the walking direction, the robot avoids the obstacle by stepping over it. Tracing performance for tar-

get value is improved by adjusting the bias of the sigmoidal function in the neuro-based algorithm. Comparison with conventional position and force hybrid control demonstrates that the neuro-based position and force hybrid control proposed in this study is highly efficient.

In the future, for walking over unstructured ground, in addition to performing force control in the x, y, z directions, we plan to perform moment control in the x, y, z directions, by means of the six-axis force sensors provided in each leg. Furthermore, for walking on a slope and unstable walking, such as dynamic walking, we plan to realize walking control consisting of position control, posture control, and force control, by employment of the proposed control.

References:

- 1) S. Hirose, K. Arikawa FDevelopment of Quadruped Walking Robot TITAN-VIII for Commercially Available Research Platform CJournal of the Robotics Society of Japan C17-8, pp.1191-1197, 1999. (in Japanese)
- 2) J. Furusho FEvolution of Research on Legged Locomotion CJournal of the Robotics Society of Japan C11-3, pp.306-313, 1993. (in Japanese)
- 3) K. Nonami, Q. Huang, D. Komizo, N. Shimoi, H. Uchida : Humanitarian Mine Detection Six-legged Walking Robot, The Third Int. Conf. on Climbing and Walking Robots, Madrid, Spain, pp.861-867, 2000.
- 4) T. Kubota, H. Katoh, I. Nakatani : Walking Rover with Multiple Legs for Planetary Exploration, Proc. of 3th International Conference on Climbing and Walking Robots , pp.795-788, 2000.
- 5) David Wettergreen, Chuck Thorpe : Developing Planning and Active Control for a Hexapod Robot, Proc. 1996 IEEE Int. Conf. on Robotics and Automotion, pp.2718-2723, 1996.
- 6) David Wettergreen, Chuck Thorpe : Exploring Mount Erebus by Walking Robot, Robotics and Autonomous Systems, 11, pp.171-185, 1993.
- 7) Aarne Halme, Jorma Selkainacho, Jussi Orara : A Six Legged Walking Machine for Research Purposes in Outdoor Environment, Technical Report PB92 - 198530, Helsink Univ. of Tech., Finland, 1992.
- 8) K. Nonami CQ. Huang, et al FDevelopment of Autonomous Six-Legged Walking Robot COMET-II with Power-Unit and Radio-Controlled Helicopter for Humanitarian Demining CThe 19th Annual Conference of the Robotics Society of Japan, pp.319-320., 2001. (in Japanese)
- 9) M. Kawato : Feedback-Error-Learning Neural Network for Supervised Motor Learning, Advanced Neural Computers, R. Eckmiller(Editor), pp.365-372, 1990.
- 10) J. Kodjabachian, J.A. Meyer : Evolution and Development of Nerural Controllers for Locomotion, Gradient-Following, and Obstacle-Avoidance in Artificial Insects, IEEE Transactions on Neural Network, 9-5, 1998.
- 11) K. Koyama and K. Nonami : Dynamic Walking Control of Quadruped Locomotion Robot Using Neural Network, Trans. of the Japan Society of Mechanical Engineers, C, 62(596), pp.1519-1526, 1996. (in Japanese)
- 12) K. Nonami, Q. Huang :Humanitarian Mine Detection Six-Legged Walking Robot COMET-II with Two Manipulators, Proc. of 4th International Conference on Climbing and Walking Robots , Karlsruhe, Germany, pp.989-996, 2001.
- 13) M. H. Raibert and J. J. Craig : Hybrid Position/Force Control of Manipulators, ASME Journal of Dynamic Systems, Measurement, and Control, 103-2, pp.126-133., 1981.



Name:

Qing-Jiu Huang

Affiliation:

Ph.D student, Division of Artificial System Science, Graduate School of Science and Technology, Chiba University

Address:

1-33 Yayoi-cho, Inage-ku, Chiba, 263-8522 Japan

Brief Biographical History:

1992- Joined Measuring Institute of China, Wuhan City, Hubei province of China
1998- Master student, Graduate School of Science and Technology, Chiba University
2000- Ph.D student, Graduate School of Science and Technology, Chiba University

Main Works:

- "CAD Model Based Autonomous Locomotion of Quadruped Robot by Using Correcting of Trajectory Planning with RNN", Qing-Jiu Huang, Kenzo Nonami, Hiroaki Uchida, Yoshihiko Iguchi, Takaaki Yanai, Special Issue on Frontiers of Motion and Vibration Control, JSME International Journal

Membership in Learned Societies:

- The Japan Society of Mechanical Engineers
- The Robotics Society of Japan



Name:

Kenzo Nonami

Affiliation:

Professor of Department of Electronics and Mechanical Engineering at Chiba University

Address:

1-33 Yayoi-cho, Inage-ku, Chiba, 263-8522 Japan

Brief Biographical History:

1980 - Research Associate, Chiba University
1988 - Associate Professor, Chiba University
1994 - Professor, Chiba University

Main Works:

- "Sliding Mode Control," Corona Pub. 1994.
- "Control System Design by MATLAB," Tokyo Denki Univ. Press, 1998.
- "Fundamental Theory of Control," Tokyo Denki Univ. Press 1998.
- "Mechanical Dynamics," Kyoritsu Pub, 1998.

Membership in Learned Societies:

- The Japan Society of Mechanical Engineers
- The Robotics Society of Japan
- IEEE, The Japan Society of Instrumentation and Control Engineers